

Two-Step Purification of Pathogenesis-Related Proteins from Grape Juice and Crystallization of Thaumatin-like Proteins

STEVEN C. VAN SLUYTER,^{§,#} MATTEO MARANGON,[§] SAMUEL D. STRANKS,[§]
KARLIE A. NEILSON,[†] YOJI HAYASAKA,[§] PAUL A. HAYNES,[†] R. IAN MENZ,^{||} AND
ELIZABETH J. WATERS^{*,§}

[§]The Australian Wine Research Institute, P.O. Box 197, Glen Osmond, SA 5064, Australia, [#]School of Botany, The University of Melbourne, Melbourne, Australia, [†]Department of Chemistry and Biomolecular Sciences, Macquarie University, Sydney, Australia, and ^{||}School of Biological Sciences, Flinders University, Adelaide, Australia

Grape thaumatin-like (TL) proteins and chitinases play roles in plant–pathogen interactions and can cause protein haze in white wine unless removed prior to bottling. A two-step method is described that highly purified hundreds of milligrams of TL proteins and chitinases from two juices by strong cation exchange (SCX) and hydrophobic interaction chromatography (HIC). The method was fast and separated isoforms of TL proteins and chitinases from within the same juice, in most cases to >97% purity. The isolated proteins were identified by peptide nanoLC-MS/MS and crystallized using a high-throughput screening method. Crystals from three protein fractions produced high-resolution X-ray crystallography data.

KEYWORDS: Protein; grape juice; wine; HIC; *Vitis vinifera*; thaumatin-like; chitinase; crystallography

INTRODUCTION

Thaumatin-like (TL) proteins and chitinases are the predominant proteins in grape (*Vitis vinifera*) juice and unfinned white wine (1). The two classes of proteins are historically considered to be pathogenesis-related (PR) proteins, although they are constitutively expressed during berry ripening and reach high concentrations regardless of pathogen presence (1–3). Grape PR proteins are of interest in plant pathology because they inhibit fungi in vitro (3), although the mechanism of inhibition is poorly understood. Grape PR proteins are of interest to wine researchers because they persist through the winemaking process and, unless removed prior to bottling, can cause undesirable hazes in white wines postbottling (4).

In nearly all commercial winemaking, grape proteins are removed with bentonite, a clay cation exchanger that binds proteins and loosely settles to the bottoms of wine tanks. The wine supernatant is then removed and filtered before bottling, leaving behind bentonite lees that normally contain 3–10% of the original wine volume (4). Wine is recovered from bentonite lees through extensive filtering or centrifugation; both processes are laborious and possibly degrade wine quality. Other bentonite-associated costs include occupational health and safety issues, waste disposal, and interference with increasingly common membrane-based winemaking technologies (4, 5). Alternatives to bentonite include other adsorbents (6, 7), ultrafiltration (8), and proteases (9), but no alternative has so far proven to be sufficiently cost-effective.

Improving bentonite usage or developing bentonite alternatives to protein haze prevention requires a thorough understanding

of the mechanisms of grape PR protein precipitation, of binding properties with respect to bentonite and other materials, and of the structural characteristics responsible for stability during winemaking and instability postbottling. Purified grape proteins are necessary for such investigations, and there have been significant efforts devoted to developing methods for purifying or fractionating grape PR proteins on preparative scales in the past. These have included ammonium sulfate precipitation (10) and ion exchange chromatography (2, 9, 11, 12). More recently, Marangon et al. (13) used hydrophobic interaction chromatography (HIC) to fractionate ammonium sulfate precipitated grape juice and wine proteins on a semipreparative scale. Despite the excellent separation of grape and wine proteins by Marangon et al. using HIC, the use of HIC for grape protein had been described only once previously (14).

In the present paper, a method is described that employs HIC on a preparative scale following grape juice protein capture and prefractionation by strong cation exchange chromatography (SCX) in place of ammonium sulfate precipitation. Used together, SCX and HIC were convenient, fast, and effective. Hundreds of milligrams of highly purified TL proteins and chitinases were isolated from Semillon and Sauvignon blanc juices. Following purification, three of the TL proteins were crystallized by a high-throughput screening method and used to produce high-resolution X-ray diffraction data. To our knowledge, the study of grape PR proteins from a structural point of view has never been attempted and could be crucial in guiding the development of alternative technologies to bentonite.

MATERIALS AND METHODS

Protein HPLC. Protein concentrations and purity were determined by reverse-phase HPLC with a Vydac 2.1 × 250 mm C8 column (208TP52 Grace Davison Discovery Sciences) on an Agilent 1200 system according

*Corresponding author (telephone +61 8 8303 6600; fax +61 8 8303 6601; e-mail elizabeth.waters@awri.com.au).

to the method of Marangon et al. (13) with minor modifications. The flow rate was 0.25 mL/min, samples were adjusted to 10% CH₃CN and 0.1% trifluoroacetic acid prior to loading in a temperature-controlled auto-sampler at 4 °C, injection volumes were 15–30 μ L, and the eluent composition was returned to equilibration conditions at 32 min.

Sodium Dodecyl Sulfate–Polyacrylamide Gel Electrophoresis (SDS-PAGE). SDS-PAGE was performed with NuPage 4–12% Bis-tris, 1.5 mm thick, 15-well gels (Invitrogen) and an XCell SureLock Mini Cell (Invitrogen) following the manufacturer's instructions. Approximately 50 mg of Na₂S₂O₅ was added to the top reservoir prior to running to prevent cysteine oxidation. Samples were prepared by diluting purified protein into sample buffer (Invitrogen NuPage recipe) with 5% 2-mercaptoethanol and boiling for 5 min. Precision Plus Protein unstained standards were from Bio-Rad. Gels were fixed for 10 min in 50% methanol/5% acetic acid and then stained with Imperial Protein Stain (Pierce) according to the manufacturer's microwave instructions with an extended incubation in stain to increase sensitivity.

Peptide NanoLC-MS/MS and Database Searching. Bands from SDS-PAGE were excised and used for peptide nanoLC-MS/MS according to the method of Marangon et al. (13) except that a ThermoFinnigan LTQ XL linear ion trap mass spectrometer was used in place of an LCQ Deca mass spectrometer. To create a grape protein database all 79,603 *V. vinifera* protein entries in NCBI were downloaded on April 16, 2009, and the FASTA file was converted to Xbang pro-FASTA format using fasta_pro.exe from the 20080801 win32 GPM-XE package freely available from thegpm.org. Database/reverse database searches were performed using the GPM Manager and X!Tandem from the GPM-XE package. Carbamidoethyl was considered to be a complete cysteine modification; oxidation of methionine and tryptophan and deamidation of asparagine and glutamine were considered to be partial modifications. Default settings in the ion trap predefined method were unchanged, including a 0.4 Da fragment mass error, with the following exceptions: peptide log(e) was < -2, protein log(e) was < -9, annotations and polymorphisms were not used during refinement, the valid expectation threshold for refinement was -5, and redundant spectra were set to be removed using the default threshold. No search returned a positive reverse database result.

Protein Electrospray Ionization Mass Spectrometry (ESI-MS). Masses of purified proteins were determined according to the method of Hayasaka et al. (15) with modifications. A 2.1 mm C8 guard column was used as a protein trap (Vydac 208GD52, Grace Davison Discovery Sciences) and eluted with gradients from 90% A (2% formic acid) to 80% B (2% formic acid in CH₃CN) at a flow rate of 0.2 mL/min directly into a 4000 Q TRAP hybrid tandem mass spectrometer equipped with a turbo ionspray source (Applied Biosystems/MDS Sciex). The ion source parameters were 5500 V for ion spray voltage, 60 V for declustering potential, 10 V for entrance potential, 40 psi for gas 1 (nebulizer) and gas 2 (turbo), 10 psi for curtain gas, and 400 °C for turbo gas temperature. Nitrogen gas was used for the curtain, nebulizer, and turbo gases. Positive ion mass spectra were recorded in a mass range from *m/z* 1200 to 2700 with a step size of 0.1 amu and a scan time of 2.0 s.

Protein Purification. Two clarified juices, a 2005 Semillon and a 2007 Sauvignon blanc, were provided by commercial wineries in South Australia and stored at -20 °C until use.

Juices (8 L of Semillon or 19 L of Sauvignon blanc; approximately 2 g total protein each) were adjusted to pH 3.0 with HCl and treated with 30 g/L polyvinylpyrrolidone (Polyclar VT and Polyclar Super R, ISP Pty Ltd.) overnight at 4 °C. Juices were filtered by vacuum through three layers of Mira cloth (Merck) and then 0.8/0.2 μ m VacuCap 90 PF filter units (Pall Corp.).

All chromatographic steps were at room temperature. Filtered juice was loaded at 8–18 mL/min with a peristaltic pump on an XK 50 column (5 cm diameter, Amersham Biosciences) packed with 175 mL of Macro-Prep High S resin (Bio-Rad) previously equilibrated with 30 mM sodium citrate, pH 3.0. The column was then connected to an ÄKTA Prime chromatography system with UV detector (Amersham Biosciences) and washed at 20 mL/min with 1.7 L of 30 mM sodium citrate, pH 3.0. Bound proteins were eluted at 20 mL/min with 30 mM MES/1 M NaCl, pH 6.0 (buffer B) using the following gradient: 0 min, 5% B; 90 min, 30% B, then to 100% B, and held. For the Semillon juice the step to 100% B was immediate; a 5 min gradient was used for the Sauvignon blanc juice.

Strong cation exchange (SCX) fractions were pooled on the basis of elution profiles at 280 nm absorbance (see chromatograms in Figure 1), adjusted to pH 5.0 (NaOH) and 1.25 M ammonium sulfate with 3.5 M ammonium sulfate, filtered (0.45 μ m Supor PES membranes, Pall Corp.), and loaded at 10 mL/min on a 110 mL, 2.6 cm diameter Phenyl Sepharose HP column (GE Healthcare) pre-equilibrated with 0.3 L of 50 mM sodium citrate containing 1.25 M ammonium sulfate, pH 5.0. When ammonium sulfate additions to SCX fractions produced precipitate, additional ammonium sulfate was added to 80% saturation and stirred overnight at 0 °C, the precipitate was collected by centrifugation, and the resulting pellets were dissolved in 50 mM sodium citrate containing 1.25 M ammonium sulfate, pH 5.0, for loading on the HIC column. The column was washed with 0.2 L of 50 mM sodium citrate containing 1.25 M ammonium sulfate, pH 5.0, and eluted with a 110 min gradient at 10 mL/min to 50 mM sodium citrate, pH 5.0.

HIC fractions (50 mL each) were pooled on the basis of elution profiles at *A*₂₈₀ and reverse-phase HPLC analysis. Ammonium sulfate concentrations of the pooled HIC fractions were calculated on the basis of elution times and were then adjusted to 90% saturation at 0 °C. Proteins were either stored as ammonium sulfate suspensions at 4 °C or collected by centrifugation, dissolved in 0.1 M malic acid, pH 3.5 (KOH), and desalted with a 11 \times 2.6 cm Bio-Gel P-4 (fine, Bio-Rad) column at 1–2 mL/min. Desalted fractions were pooled on the basis of conductivity and *A*₂₈₀ and stored at -80 °C.

Crystallization. Proteins were concentrated by ultrafiltration (Nanosep 3k, Pall Corp.) in 5 mM formic acid, 10 mM NaCl. Screening to identify crystallization conditions was performed by the sitting-drop vapor diffusion method using five Nextal screening kits (Anions, Cations, Pegs, Classics, and Cryos from Qiagen) and Intelliplate 96-2 (Hampton Research) loaded with a Phoenix crystallization robot (Art Robbins Instruments). Equal volumes of protein and reservoir solutions (0.2 μ L + 0.2 μ L in the large well, 0.1 μ L + 0.1 μ L in the small well) were mixed and equilibrated against 100 μ L of reservoir solution at 20 °C. For each protein, five crystallization plates were incubated and imaged in a CrystalPro Microscope (Tritek) with motorized stage and automatic image capture and storage. Secondary screens and optimizations were performed in 24-well Cryschem plates (Hampton Research) to obtain diffracting crystals. Equal volumes of protein and reservoir solution (1.5 μ L + 1.5 μ L) were mixed and equilibrated against 500 μ L of reservoir solution at 20 °C. Crystals were harvested into appropriate harvest solutions (see Results and Discussion, Table 2) and progressively transferred to harvest solutions with glycerol concentrations increasing in 5% steps. Crystals in harvest solution containing 20% glycerol were frozen by plunging in liquid nitrogen (16).

X-ray Crystallography. Data were collected from single cryocooled (100 K) crystals that were either robotically mounted on beamline PX1, controlled using Blu-Ice software (17), or manually loaded on beamline PX2 at the Australian Synchrotron, Victoria, Australia. Diffraction images were collected on Area Detector Systems Corp. CCD detectors. The diffraction data were analyzed using MOSFLM interfaced by IMOSFLM (18).

RESULTS AND DISCUSSION

Previous grape PR protein purification strategies from juice or wine have used either ammonium sulfate precipitation (2, 10, 13) or cation exchange (12, 19) as initial concentration steps. Cation exchange was used in this study to avoid using large amounts of ammonium sulfate and to provide a convenient method for fractionating captured proteins. Cation exchange at grape juice pH binds the majority of grape PR proteins but generally does not bind grape-derived polysaccharides, which tend to be either negatively charged or neutral (20), and has the added advantage of doing so at a pH value close to those of juice and wine. The SP Sepharose column of Muhlack et al. (12) was replaced with polyacrylamide-based Bio-Rad Macro-Prep High S to allow higher linear flow rates and potentially reduce nonspecific interactions of PR proteins with polysaccharide-based gels.

Volumes of juice loaded on the SCX column were based on an expected binding capacity of at least 10 mg of protein/mL of

Table 1. Purified Protein Characteristics

protein ^a	HPLC		X!Tandem ^b			theoretical ^d			measured mass ^e	
	yield (mg)	% purity	top ranked protein	peptides matched	log(e)	top annotated BlastP result (identities) ^c	SignalP cleavage site	MW		pI
A [⊥]	365	>99	gil33329392 gb AAQ10093.1 class IV chitinase [<i>Vitis vinifera</i>]	168	-1480.6		AVA-QN	25617	5.15	25633
B	175	>99	gil33329390 gb AAQ10092.1 thaumatin-like protein [<i>Vitis vinifera</i>]	41	-441.3		SYA-AT	21276	4.54	21263
C [*]	220	98	gil7406716 emb CAB85637.1 putative thaumatin-like protein [<i>Vitis vinifera</i>]	60	-287.9		HEA-TF	21240	4.76	21253
D1 [§]	150	69	gil157353734 emb CAO46266.1 unnamed protein product [<i>Vitis vinifera</i>]	15	-217.9	gil164699029 gb ABY66957.1 class IV chitinase [<i>Vitis pseudoreticulata</i>] (204/264)	not predicted	34680	7.47	25930
D2 [*]	40	88	gil7406716 emb CAB85637.1 putative thaumatin-like protein [<i>Vitis vinifera</i>]	56	-346.8		HEA-TF	21240	4.76	21253
F1 [⊥]	190	>99	gil33329392 gb AAQ10093.1 class IV chitinase [<i>Vitis vinifera</i>]	162	-1322.3		AVA-QN	25617	5.15	25634
F2	100	90	gil225426793 ref XP_002282964.1 PREDICTED: hypothetical protein [<i>Vitis vinifera</i>]	57	-558.1	gil33329390 gb AAQ10092.1 thaumatin-like protein [<i>Vitis vinifera</i>] (223/225)	SYA-AT	21252	4.54	21241
G [‡]	400	>99	gil2213852 gb AAB61590.1 VVTL1 [<i>Vitis vinifera</i>]	66	-334.4		THA-AT	21287	4.76	21275
H1 [§]	20	91	gil157353734 emb CAO46266.1 unnamed protein product [<i>Vitis vinifera</i>]	18	-270.8	gil164699029 gb ABY66957.1 class IV chitinase [<i>Vitis pseudoreticulata</i>] (204/264)	not predicted	34680	7.47	25932
H2 [‡]	30	>99	gil2213852 gb AAB61590.1 VVTL1 [<i>Vitis vinifera</i>]	51	-278.6		THA-AT	21287	4.76	21274
I [‡]	180	>99	gil2213852 gb AAB61590.1 VVTL1 [<i>Vitis vinifera</i>]	46	-267.6		THA-AT	21287	4.76	21275

^a Protein names were assigned on the basis of SCX (letters) and HIC fractions (numbers; no number indicates that the associated SCX fraction yielded one major protein by HIC). Superscript symbols indicate identical X!Tandem top ranked results. ^b Tryptic peptide mass spectra were assigned by X!Tandem to entries in a database of *Vitis vinifera* protein sequences. Supporting Information Figure S2 indicates sequence coverage by nanoLC-MS/MS data. ^c In cases when X!Tandem top ranked proteins were not functionally annotated, the associated sequences were compared to NCBI nr using BlastP (blast.ncbi.nlm.nih.gov). Identities refer to the number of matching amino acids of the X!Tandem result (numerator) to the number of amino acids in the sequence associated with the BlastP result (denominator). ^d Sequences associated with X!Tandem results were analyzed by SignalP to find signal peptide cleavage sites (www.cbs.dtu.dk/services/SignalP) (26). Theoretical average MW and pI were calculated with the ExPASy-Compute pI/MW tool using sequences excluding theoretical signal peptides (au.expasy.org/tools/pi_tool.html). ^e Intact protein masses were determined by ESI-MS.

High S. In preliminary trials we found that binding capacity decreased with increasing linear flow rates (not shown), but the 5 cm diameter column used for SCX allowed flow rates up to 18 mL/min without apparently exceeding the binding capacity of the column. For example, in the case of the Sauvignon blanc juice, at the end of the 19 L sample load of approximately 1800 mg of protein per 175 mL column volume, the eluent contained 7.0 mg of protein/L and only 1.1 mg/L was potentially protein of interest as determined by HPLC (not shown).

Following a wash with low ionic strength, pH 3.0, buffer, proteins were eluted from the SCX column with a pH and salt gradient (**Figure 1**). Although the chromatograms for the two juices are roughly similar, showing two major peaks in the initial gradient followed by a third major peak eluting with the step to high salt, the retention times for the Semillon peaks are longer than those for Sauvignon blanc. The two starting juice volumes could explain the differences in elution time, the larger volume of Sauvignon blanc juice moving bound proteins down the column. Additionally, matrix effects might explain the differences. For

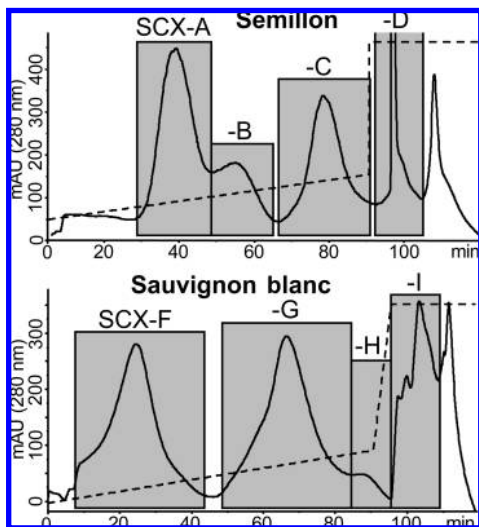


Figure 1. Cation exchange chromatograms for two juices on a 5 cm diameter, 175 mL, Bio-Rad Macro-Prep High S column. Both chromatograms begin at the start of the gradient to high salt; they omit the loads and washes. The dotted line indicates the salt/pH gradient. The peak associated with SCX-D exceeded 2000 mAU. Approximately 8 L of Semillon juice and 19 L of Sauvignon juice were loaded, 2200 mg of protein and 1800 mg of protein, respectively. Collected fractions (shaded) SCX-A to -D and SCX-F to -I were used for HIC.

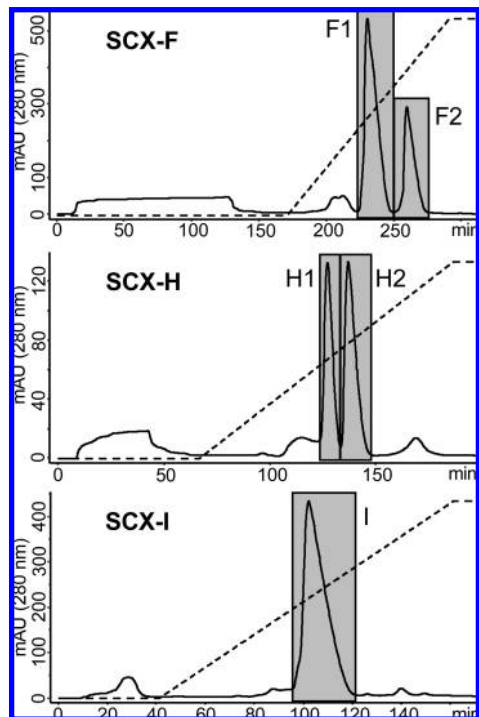


Figure 2. HIC chromatograms for SCX fractions F, H, and I. Assigned names for purified proteins are shown next to the associated shaded peaks. HIC was performed on a 2.6 cm diameter 110 mL Phenyl Sepharose HP column. SCX fractions were adjusted to 1.25 M ammonium sulfate prior to loading on the column; SCX-I was precipitated before dissolving in buffered 1.25 M ammonium sulfate. Different load and wash times prior to the start of the gradient to low salt reflect the different sample volumes for the different fractions.

both juices, when the SCX column was washed with water and then 20% ethanol after eluting proteins, nonprotein compounds eluted that absorbed strongly at 280 nm (not shown). Similarly,

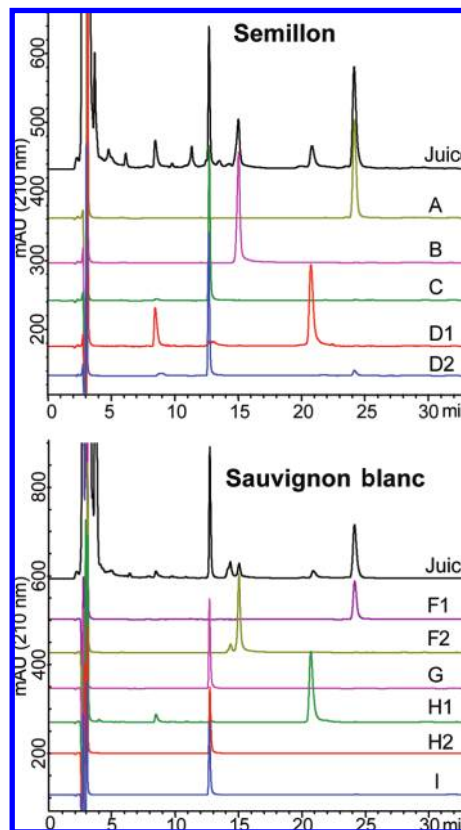


Figure 3. Reverse phase (C8) HPLC chromatograms of HIC purified proteins and starting juices. Peak areas do not reflect purification yields.

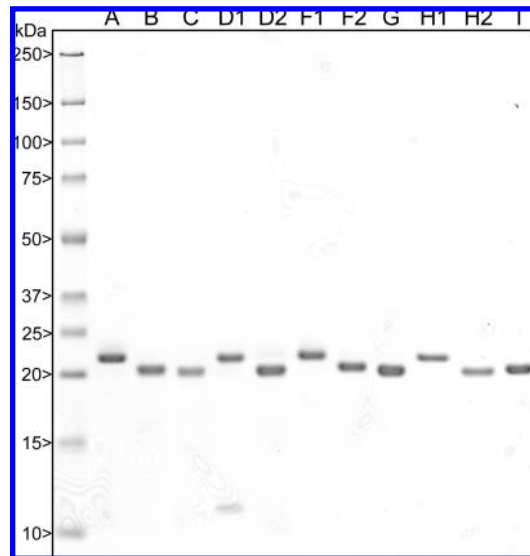
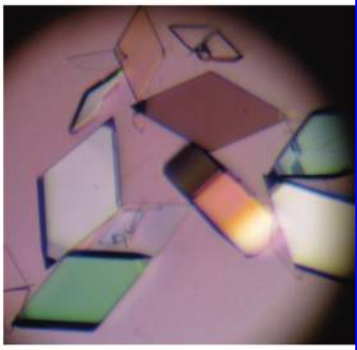




Figure 4. Purified proteins ($\sim 0.7 \mu\text{g}$ per lane) were reduced, subjected to SDS-PAGE, and visualized with Coomassie R-250.

the majority of the 280 nm absorbance in SCX fractions associated with the unshaded, late-eluting peaks in **Figure 1** was attributable by reverse-phase HPLC to apparent phenolic compounds with absorbance maxima ranging from 310 to 320 nm; proteins, as determined by local absorbance maxima from 275 to 280 nm, were present in low concentrations (not shown). The nonprotein compounds could be grape phenolics that bind nonspecifically to the column and influence protein retention time, depending on the starting material.

Table 2. Crystallization Conditions

Protein	Initial concentration	Crystal growing conditions	Harvest solutions	Crystal image
F2	12 mg/mL	0.1 M Na acetate pH 4.6 6% PEG 4000 10 mM MgCl ₂	55 mM Na acetate pH 4.6 4.4% PEG 4000 5.5 mM MgCl ₂ 2.75 mM formic acid 5.5 mM NaCl	
H2	20 mg/mL	2.58 M Mg acetate 0.2 M MES	1.375 M Mg acetate 55 mM MES 2.25 mM formic acid 4.5 mM NaCl	
I	28 mg/mL	2 M Mg acetate 0.1 M Na acetate pH 4.6	1.1 M Mg acetate 55 mM Na acetate pH 4.6 2.75 mM formic acid 5.5 mM NaCl	

Pooled SCX fractions were further fractionated by hydrophobic interaction chromatography (HIC) on Phenyl Sepharose HP. In HIC, high kosmotropic salt concentrations promote protein binding and protein is eluted with a gradient to decreasing salt. HIC was a convenient step following SCX because the high salt in the SCX fractions does not interfere with HIC, large-volume SCX fractions may be loaded, and the mechanisms of separation are orthogonal; that is, SCX separates on the basis of surface charge, which is unrelated to surface hydrophobicity.

Three examples of HIC purifications of SCX fractionated proteins are shown in **Figure 2**; Supporting Information Figure S1 contains the remaining HIC chromatograms. **Table 1** contains data on purities, yields, and identities for the HIC purified proteins. By using an approach that is becoming more frequently used in grape and wine protein studies (13, 21–23), protein identity was determined on the basis of nanoLC-MS/MS of tryptic peptides and database searching. The resulting sequences likely represent homologues and not the actual sequences of the purified proteins in most cases because of the inherent limitations of available grape protein sequences (primarily Pinot noir sequences and few, if any, Semillon and Sauvignon blanc sequences) and the high heterozygosity of grapes (24). In several cases the theoretical MW was close to the measured mass, and differences could perhaps be explained by incorrect signal peptide predictions, disulfide bonding, or other post-translational modifications. However, such analysis is beyond the scope of the presented work and the nanoLC-MS/MS data do not provide complete coverage of any sequence. Therefore, it is not suggested

that the purified proteins exactly match corresponding database entries. Solved crystal structures will make possible comparisons between purified proteins and database entries.

HIC with Phenyl Sepharose SP was very effective in separating TL proteins from chitinases. For example, fractions F1 and H1 contain chitinases, and F2 and H2 contain TL proteins. The longer HIC retention times of TL proteins as compared to chitinases correspond with the general trend found by Marangon et al. (13) using the same packing material for semipreparative fractionation of grape juice and wine proteins. In addition to excellent resolution of TL proteins and chitinases, HIC purified to 98% or higher either TL proteins or chitinases from seven of the eight SCX fractions collected from the two juices. Purities of pooled HIC fractions are demonstrated by HPLC (**Figure 3**) and SDS-PAGE (**Figure 4**). Only in one case, SCX-D, did HIC fail to highly purify a chitinase or TL protein. In the case of protein D1 the low MW contaminating protein visible by SDS-PAGE was identified by peptide nanoLC-MS/MS as a lipid transfer protein (see Supporting Information Table S1). The contaminant in protein D2 is visible by SDS-PAGE as a faint band at ~22 kDa and is most likely a chitinase. The only other case of a potentially contaminating protein being subjected to SDS-PAGE and peptide nanoLC-MS/MS was in the HIC separation of SCX-G (**Figure S1**). A peak that eluted after protein G was found to contain an apparent vacuolar invertase (**Table S1**).

In addition to demonstrating protein purity, the HPLC chromatograms in **Figure 3** suggest a trend among the protein purifications of both juices. In both cases the major chitinases

Table 3. X-ray Data Collection Statistics

parameter	protein F2	protein H2	protein I
beamline	PX1	PX2	PX1
resolution (Å)	1.2	1.8	1.8
space group	P222	C2	C2
unit-cell parameters (Å)			
<i>a</i>	34.99	122.48	122.21
<i>b</i>	70.31	52.61	52.73
<i>c</i>	75.25	91.67	94.39

(A and F1) elute early from SCX. In the case of the Sauvignon blanc juice a TL protein (F2) coelutes by SCX with the first chitinase; the corresponding Semillon protein (B) was partially separated by SCX. The major proteins of the second large SCX fraction in both cases were TL proteins C and G. The next proteins to elute by SCX, the D and H proteins, in both cases seem to be a second chitinase and the major TL protein carried over from the previous fraction.

A significant difference between the two separations is protein I from Sauvignon blanc and the lack of a corresponding protein in Semillon. Interestingly, the X!Tandem identities are the same (VvTL1) for proteins G, H2, and I even though there is considerable separation between SCX fractions G and I. Also, the measured masses were not significantly different among the three proteins ($n = 6$). Tattersall et al. (2) reported the mass of VvTL1 to be 21272.90 and suggested that the difference between the observed mass and predicted mass (14 amu) was caused by disulfide bonding. Also, the crystal structure of a banana TL protein homologous to grape TL proteins includes eight disulfide bonds (25). Similarly abundant disulfide bonds are likely present in the TL proteins isolated in this study. It is possible that variations in disulfide bonding could be reflected in conformational differences, even among proteins with identical primary structure, that lead to different SCX retention times and crystallization conditions (e.g., proteins H2 and I, see below, **Table 2**). Solving the crystal structures of proteins H2 and I should resolve differences in disulfide bonding.

Thaumatococcus-like proteins F2, H2, and I were subjected to high-throughput screens to establish crystallization conditions. Five Qiagen screening kits of 96 conditions each were used in duplicate for each protein. The process was facilitated greatly by a liquid handling robot that delivered small volumes of proteins and precipitants to 96-well plates that were then observed regularly by a separate imaging robot so that stored images could be viewed remotely and in bulk. Initial conditions that produced evidence of protein crystallization were modified to produce concentration ranges of individual components in subsequent manual and larger volume screens. Seventy-two crystals of the three proteins were produced and analyzed on beamline PX1 at the Australian Synchrotron; many showed some level of X-ray diffraction. The crystallization conditions that produced the best diffracting crystals for each protein are shown in **Table 2**; **Table 3** summarizes the diffraction data. The different isoforms produced crystals of two different space groups, C2 and P222, and unit cell dimensions. Many of the crystals were small (less than 40 μm) which resulted in the protein H2 crystal only producing high resolution diffraction data on the microfocus beamline PX2. The space group and unit cell size of protein F2 are very similar to those obtained for a banana TL protein (25).

In addition to crystal production we have used and continue to use the purified PR proteins in pathogen bioassays (27), as substrates in protease assays, for protein precipitation kinetics studies (28), and for protein melting experiments. Also, when the high similarity of grape PR proteins with PR proteins of other plant species is considered, working with grape PR proteins in

studies of other plants could be useful because of the abundant supply of grape juice and its ease of use.

The two-step purification scheme is simple, fast, and capable of generating large amounts of highly purified proteins under non-denaturing conditions. Strong cation exchange allows the capture and fractionation of proteins at grape juice pH, and HIC provides a complementary method that is very capable of resolving PR proteins. The method is a significant improvement over previous methods because it is non-denaturing (unlike anion exchange or chitin affinity methods) and simultaneously purifies TL proteins and chitinases. In addition to the purification method, high-throughput robotics facilitated crystallization condition screening so that several proteins could be screened in parallel and subjected to X-rays for structural determinations to be published.

ABBREVIATIONS USED

TL, thaumatococcus-like; SCX, strong cation exchange; HIC, hydrophobic interaction chromatography; PR, pathogenesis-related; MES, 2-morpholinoethanesulfonic acid; MW, molecular weight; *pI*, isoelectric point; PX1, high-throughput protein crystallography beamline; PX2, protein microcrystal and small molecule X-ray diffraction beamline; C2, centered monoclinic; P222, primitive orthorhombic.

ACKNOWLEDGMENT

This research was undertaken on the PX1 and PX2 beamlines at the Australian Synchrotron, Victoria, Australia. The views expressed herein are those of the authors and are not necessarily those of the owner or operator of the Australian Synchrotron. We thank Professor Antony Bacic, Dr. Filomena Pettolino, and Professor John Carver for their advice and support. We thank Dr. Tom Caradoc-Davies, Ruth Plathe, and Drew Sutton for assistance with X-ray diffraction data collection.

Supporting Information Available: Additional HIC chromatograms (Figure S1), identifications of two unpurified proteins (Table S1), and sequence coverage of nanoLC-MS/MS data (Figure S2). This material is available free of charge via the Internet at <http://pubs.acs.org>.

LITERATURE CITED

- Pocock, K. F.; Hayasaka, Y.; McCarthy, M. G.; Waters, E. J. Thaumatococcus-like proteins and chitinases, the haze-forming proteins of wine, accumulate during ripening of grape (*Vitis vinifera*) berries and drought stress does not affect the final levels per berry at maturity. *J. Agric. Food Chem.* **2000**, *48*, 1637–1643.
- Tattersall, D. B.; van Heeswijk, R.; Høj, P. B. Identification and characterization of a fruit-specific, thaumatococcus-like protein that accumulates at very high levels in conjunction with the onset of sugar accumulation and berry softening in grapes. *Plant Physiol.* **1997**, *114*, 759–769.
- Salzman, R. A.; Tikhonova, I.; Bordelon, B. P.; Hasegawa, P. M.; Bressan, R. A. Coordinate accumulation of antifungal proteins and hexoses constitutes a developmentally controlled defense response during fruit ripening in grape. *Plant Physiol.* **1998**, *117*, 465–472.
- Waters, E. J.; Alexander, G.; Muhlack, R.; Pocock, K. F.; Colby, C.; O'Neill, B. N.; Høj, P. B.; Jones, P. R. Preventing protein haze in bottled white wine. *Aust. J. Grape Wine Res.* **2005**, *11*, 215–225.
- Salazar, F. N.; de Bruijn, J. P. F.; Seminario, L.; Güell, C.; López, F. Improvement of wine crossflow microfiltration by a new hybrid process. *J. Food Eng.* **2007**, *79*, 1329–1336.
- Sarmento, M. R.; Oliveira, J. C.; Boulton, R. B. Selection of low swelling materials for protein adsorption from white wines. *Int. J. Food Sci. Tech.* **2000**, *35*, 41–47.
- Salazar, F. N.; Achaerandio, I.; Labbé, M. A.; Güell, C.; López, F. Comparative study of protein stabilization in white wine using

- zirconia and bentonite: physicochemical and wine sensory analysis. *J. Agric. Food Chem.* **2006**, *54*, 9955–9958.
- (8) Hsu, J. C.; Heatherbell, D. A.; Flores, J. H.; Watson, B. T. Heat-unstable proteins in grape juice and wine. II. Characterization and removal by ultrafiltration. *Am. J. Enol. Vitic.* **1987**, *38*, 17–22.
- (9) Waters, E. J.; Wallace, W.; Williams, P. J. Identification of heat-unstable wine proteins and their resistance to peptidases. *J. Agric. Food Chem.* **1992**, *40*, 1514–1519.
- (10) Waters, E. J.; Wallace, W.; Williams, P. J. Heat haze characteristics of fractionated wine proteins. *Am. J. Enol. Vitic.* **1991**, *42*, 123–127.
- (11) Ferreira, R. B.; Monteiro, S.; Picarra-Pereira, M. A.; Tanganho, M. C.; Loureiro, V. B.; Teixeira, A. R. Characterization of the proteins from grapes and wines by immunological methods. *Am. J. Enol. Vitic.* **2000**, *51*, 22–28.
- (12) Muhlack, R. A.; Waters, E. J.; Lim, A.; O'Neill, B. K.; Colby, C. B. An alternative method for purification of a major thaumatin-like grape protein (VVTL1) responsible for haze formation in white wine. *Asia Pac. J. Chem. Eng.* **2007**, *2*, 70–74.
- (13) Marangon, M.; Van Sluyter, S. C.; Haynes, P. A.; Waters, E. J. Grape and wine proteins: their fractionation by hydrophobic interaction chromatography and identification by chromatographic and proteomic analysis. *J. Agric. Food Chem.* **2009**, *57*, 4415–4425.
- (14) Brissonnet, F.; Maujean, A. Characterization of foaming proteins in a champagne base wine. *Am. J. Enol. Vitic.* **1993**, *44*, 297–301.
- (15) Hayasaka, Y.; Adams, K. S.; Pockock, K. F.; Baldock, G. A.; Waters, E. J.; Høj, P. B. Use of electrospray mass spectrometry for mass determination of grape (*Vitis vinifera*) juice pathogenesis-related proteins: a potential tool for varietal differentiation. *J. Agric. Food Chem.* **2001**, *49*, 1830–1839.
- (16) Pflugrath, J. W. Macromolecular cryocrystallography—methods for cooling and mounting protein crystals at cryogenic temperatures. *Methods* **2004**, *34*, 415–423.
- (17) McPhillips, T. M.; McPhillips, S. E.; Chiu, H.-J.; Cohen, A. E.; Deacon, A. M.; Ellis, P. J.; Garman, E.; Gonzalez, A.; Sauter, N. K.; Phizackerley, R. P.; Soltis, S. M.; Kuhn, P. Blu-Ice and the Distributed Control System: software for data acquisition and instrument control at macromolecular crystallography beamlines. *J. Synchrotron Radiat.* **2002**, *9*, 401–406.
- (18) Leslie, A. G. W. Joint CCP4 + ESF-EAMCB Newsletter on Protein Crystallography, No. 26. **1992**.
- (19) Canals, J. M.; Arola, L.; Zamora, F. Protein fraction analysis of white wine by FPLC. *Am. J. Enol. Vitic.* **1998**, *49*, 383–388.
- (20) Vidal, S.; Williams, P.; Doco, T.; Moutounet, M.; Pellerin, P. The polysaccharides of red wine: total fractionation and characterization. *Carbohydr. Polym.* **2003**, *54*, 439–447.
- (21) Kwon, S. W. Profiling of soluble proteins in wine by nano-high-performance liquid chromatography/tandem mass spectrometry. *J. Agric. Food Chem.* **2004**, *52*, 7258–7263.
- (22) Sarry, J. E.; Sommerer, N.; Sauvage, F. X.; Bergoin, A.; Rossignol, M.; Albagnac, G.; Romieu, C. Grape berry biochemistry revisited upon proteomic analysis of the mesocarp. *Proteomics* **2004**, *4*, 201–215.
- (23) Cilindre, C.; Jégou, S.; Hovasse, A.; Schaeffer, C.; Castro, A. J.; Clément, C.; Van Dorsselaer, A.; Jeandet, P.; Marchal, R. Proteomic approach to identify champagne wine proteins as modified by *Botrytis cinerea* infection. *J. Proteome Res.* **2008**, *7*, 1199–1208.
- (24) Velasco, R.; Zharkikh, A.; Troggo, M.; Cartwright, D. A.; Cestaro, A.; Pruss, D.; Pindo, M.; FitzGerald, L. M.; Vezzulli, S.; Reid, J.; Malacarne, G.; Iliev, D.; Coppola, G.; Wardell, B.; Micheletti, D.; Macalma, T.; Facci, M.; Mitchell, J. T.; Perazzolli, M.; Eldredge, G.; Gatto, P.; Oyzerski, R.; Moretto, M.; Gutin, N.; Stefanini, M.; Chen, Y.; Segala, C.; Davenport, C.; Demattè, L.; Mraz, A.; Battilana, J.; Stormo, K.; Costa, F.; Tao, Q.; Si-Ammour, A.; Harkins, T.; Lackey, A.; Perbost, C.; Taillon, B.; Stella, A.; Solovyev, V.; Fawcett, J. A.; Sterck, L.; Vandepoele, K.; Grando, S. M.; Toppo, S.; Moser, C.; Lanchbury, J.; Bogden, R.; Skolnick, M.; Sgaramella, V.; Bhatnagar, S. K.; Fontana, P.; Gutin, A.; Van de Peer, Y.; Salamini, F.; Viola, R. A high quality draft consensus sequence of the genome of a heterozygous grapevine variety. *PLoS ONE* **2007**, *2*, e1326.
- (25) Leone, P.; Menu-Bouaouiche, L.; Peumans, W. J.; Payan, F.; Barre, A.; Roussel, A.; Van Damme, E. J. M.; Rougé, P. Resolution of the structure of the allergenic and antifungal banana fruit thaumatin-like protein at 1.7-Å. *Biochimie* **2006**, *88*, 45–52.
- (26) Dyrlov Bendtsen, J.; Nielsen, H.; von Heijne, G.; Brunak, S. Improved prediction of signal peptides: SignalP 3.0. *J. Mol. Biol.* **2004**, *340*, 783–795.
- (27) ten Have, A.; Espino, J. J.; Dekkers, E.; Van Sluyter, S. C.; Brito, N.; Kay, J.; González, C.; van Kan, J. A. L. The *Botrytis cinerea* aspartic proteinase family. *Fungal Genet. Biol.* **2009**, doi: 10.1016/j.fgb.2009.10.008.
- (28) Stranks, S. D.; Ecroyd, H.; Van Sluyter, S.; Waters, E. J.; Carver, J. A.; von Smekal, L. Model for amorphous aggregation processes. *Phys. Rev. E* **2009**, in press.

Received for review July 9, 2009. Revised manuscript received September 9, 2009. Accepted September 22, 2009. This work was supported financially by Australia's grapegrowers and winemakers through their investment body, the Grape and Wine Research and Development Corporation, with matching funds from the Australian government.